Scientific Research Publishing

Journal of Geographic Information System, 2022, 14, 634-651
https://www.scirp.org/journal/jgis
ISSN Online: 2151-1969
ISSN Print: 2151-1950

A New Multistep Approach to Identify Leaf-Off Poplar Plantations Using Airborne Imagery

Ramzan Ali Khorrami[1*], Zahra Naeimi[2], Michael Wing[3], Hossein Ahani[4], Sayed M. Bateni[5]

[1]Forests and Rangelands Research Department, Mazandaran Agricultural and Natural Resources Research and Education Center, Agricultural Research, Education and Extension Organization (AREEO), Sari, Iran
[2]Department of Physics, University of Tehran, Tehran, Iran
[3]Forest Engineering, Resources, and Management, Oregon State University, Corvallis, OR, USA
[4]Ministry of Agriculture, Tehran, Iran
[5]Department of Civil and Environmental Engineering and Water Resources Research Center, University of Hawaii at Manoa, Honolulu, HI, USA
Email: *khorrami20166@gmail.com

How to cite this paper: Khorrami, R.A., Naeimi, Z., Wing, M., Ahani, H. and Bateni, S.M. (2022) A New Multistep Approach to Identify Leaf-Off Poplar Plantations Using Airborne Imagery. *Journal of Geographic Information System*, **14**, 634-651.
https://doi.org/10.4236/jgis.2022.146036

Received: November 11, 2022
Accepted: December 27, 2022
Published: December 30, 2022

Abstract

Identification of type of leafless trees using both fall imagery and field-based surveys is a global concern in the forest science community. Few studies were devoted to separate leafless trees from others in the growth season using remote sensing imagery. But this study was the first attempt to identify the type of leafless tree in the fall imagery. We investigated the potential of the Simple Linear Iterative Clustering (SLIC) and k-mean segmentation techniques, and texture and color image analyses to identify leafless poplar trees using imagery collected in a leaf-off season. For the first time in this study, the *star shaped* feature identifier was found through a binary image that was successful in identifying leaf-off poplar plantations. Optimal threshold values of Normalized Difference Vegetation Index (NDVI) and Normalized Green Index (NGI) indices were able to differentiate highly vegetated land, green farms, and gardens from the grasses that sometimes grow between poplar plantation lines. A Coefficient of Variation (CV) of red color intensity and histogram of value were also successful in separating bare soil and other land cover types. Imagery was processed and analyzed in a Matlab software. In this study, leafless poplar plantation was identified with a user accuracy of 84% and the overall accuracy was obtained 81.3%. This method provides a framework for identification of leafless poplar trees that may be beneficial for distinguishing other types of leafless trees.

Keywords

Leafless Poplar Plantations, Fall Ultracam Imagery, Star Shaped-Feature,

K-Mean Segmentation, Texture and Color Image Analysis

1. Introduction

Leafless trees in forests and orchards are significant indicators for monitoring environmental stresses and can also reveal phenological stages in deciduous trees [1] [2]. Therefore, the detection of leafless trees is of utmost importance and provides baseline information to better understand the outbreak and damage caused by pests, diseases, air pollution, climate change and/or management scenarios [3] [4] [5].

Leafless trees can be found through field-based surveys and could be detected using remote sensing imagery approaches [1]. Although field-based surveys have been usually used to find leafless trees, they may not be the most optimal solution due to the high cost and time required for field operations. Remote sensing-based methods offer an alternative approach to detect leafless trees over a large extent that may be a more efficient time and labor solution [6]. Current increased spatial, radiometric, and spectral resolution satellite imagery, such as WorldView-2 (WV-2), can provide improved data to detect leafless trees [1]. Given the rapid progress of very high-resolution air-borne and space-borne sensors, some attempts have recently occurred that accurately detected leafless trees using remotely sensed data. [1] separated leafless trees from different types of vegetation using WV-2 data and image processing algorithms with an overall accuracy of 87% - 89%. Also, other studies have been reported acceptable accuracies for detecting the leafless trees in forest ecosystems using Airborne Laser Scanning (ALS) data, a combination of multispectral WV-2 and ALS data, and spectral data alone [2] [7].

However, unlike leafless trees detection, identification of leafless trees type (at genus level) using both fall (leaf-off) imagery and field-based surveys is a global concern in the forest and agriculture science community due to challenges in sensing key components of crown such as leaves, flowers, fruits, and distinctive spectral reflectances [8] [9]. Generally, there is a trivial spectral difference between leafless trees and bare lands which is the most important challenge for identification of the leafless trees using the fall imagery. In the absence of the green pigment (which is essential in reflecting green and near infrared light and absorbing red and blue spectra), trees absorb energy at near-infrared wavelengths and tend to appear to be dark or gray in color. Unlike green vegetation, leafless trees do not show sharp increases in the reflectance values of the near-infrared spectrum of light and show a spectral signature similar to that of the bare soil cover [10]. This property along with the Normalized Difference Vegetation Iindex (NDVI) is usually considered as the fundamental indicators to distinguish between leafless trees and other types of vegetation [11].

In this study, we developed a multistep process analysis using the Simple Li-

near Iterative Clustering (SLIC) and *k*-mean segmentation techniques as well as Gray Level Co-occurrence Matrix (GLCM) algorithm to identify leafless poplar plantations using imagery captured a fall leaf-off time period. The proposed method can identify leafless poplar plantations based on texture and color features extracted from RGB and NIR Ultracam imagery [12]. Although well-known indices, functions, and statistical parameters (e.g. homogeneity, variance, and Coefficient of Variation (CV)) were used in this study, the application of these mathematical and statistical concepts and the establishment of threshold values is unique. We applied our methodology in an area with a vast array of poplar plantations, known as Ziabar in northern Iran. Our main objective was to identify leafless poplar plantations. In other words, not all leafless species are being covered. Features and combination conditions as well as thresholds used in this paper were presented for identification of leaf-off poplar plantations. They may also distinguish other types of leafless trees with some changes in the thresholds and conditions. Since this study was not carried on other leafless trees, it is not possible to comment on them. Preparing a distribution map or determining the size of the poplar plantation area was not our goal at all.

2. Materials and Methods

2.1. Study Area and Data

This study was carried out in the Caspian seaside lowland plains in the Ziabar region (Iran: Giulan province). A large plantation of poplar trees exists in this area which is located at 49˚7'19.63"E to 49˚23'48.87"E and 37˚22'33.95"N to 37˚30'1.37"N. The Land Cover (LC) of this region mainly consists of plowed soil, bare soil, poplar plantation, rice field, forest, grass, residential area, road networks, shallow water, and shrubs.

Airborne UltraCam digital images with a 0.1 m resolution acquired in fall season, in visible (RGB color) and Near Infra-Red (NIR) wavelengths in TIF format (without radiometric correction), were employed for the identification of leafless poplar plantations. The image included 11,310 × 17,310 pixels and the Ground Sample Distance (GSD) was 10 cm × 10 cm for all VNIR bands. A window of images having 1000 × 600 pixels arrays was subtracted from the original images by cropping them. This window moves across the image and all processes and analyses were conducted in the moving window area. Imagery was processed and analyzed in a Matlab software.

2.2. Image Properties

Following image properties are required for our image analyze and process.

2.2.1. RGB Color and NIR Spectral Band

Based on the color matrices, we extracted more information from the images by using different spectral indices based on visible and NIR spectra which were clarified as follows:

1) Normalized indices:

$$\text{Normalized Red Index (NRI)} = \frac{R}{R+G+B} \quad (1)$$

$$\text{Normalized Green Index (NGI)} = \frac{G}{R+G+B} \quad (2)$$

$$\text{2) Normalized Difference Vegetation Index (NDVI)} = \frac{NIR-R}{NIR+R} \quad (3)$$

2.2.2. Texture

Texture is a visual pattern delineation that requires more than the presence of a single color or intensity. Texture can provide key information about the structural arrangement of surfaces and their relationship with their surrounding environment [13] [14]. We considered different approaches to texture delineation in our imagery depending on land cover type. A few types of textures which exist within the image LCs of the study area are illustrated in **Figures 1(a)-(d)**.

Histogram

The histogram of a digital image with intensity levels in the range [0, $L-1$] is a discrete function [15].

$$h(r_k) = n_k \quad (4)$$

where r_k is the k_{th} gray level, n_k is the number of pixels in digital image having r_k and $h(r_k)$ is the histogram of the digital image with gray level r_k.

Three major stages (described below) including image pre-processing, image segmentation and non-poplar separating are required before identifying leafless poplar plantation can occur and are described below.

2.3. Image Pre-Processing

Linear contrast stretch using decorrelation stretch method

Decorrelation stretching enhances the color separation of an image with significant band-to-band correlation [16]. The resulting decorrelated image has a

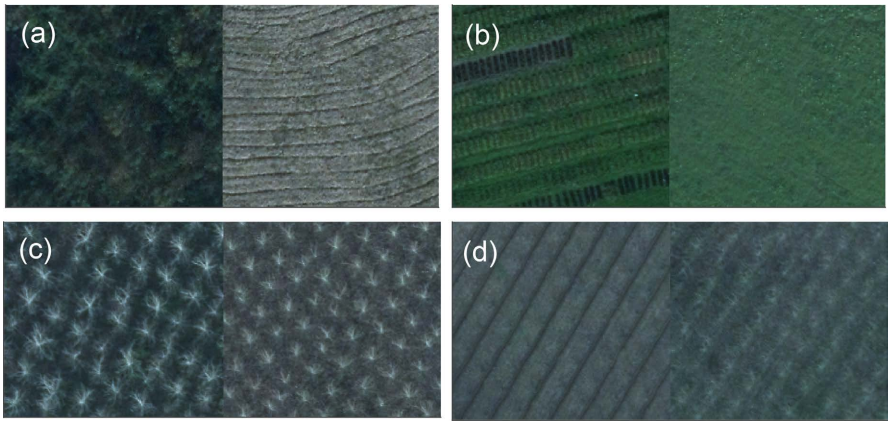

Figure 1. (a) Two types of LCs with different color and texture; (b) Two types of LCs with same color and different texture; (c) One type of LC with different color and same texture; (d) Two types of LCs with the same texture and color.

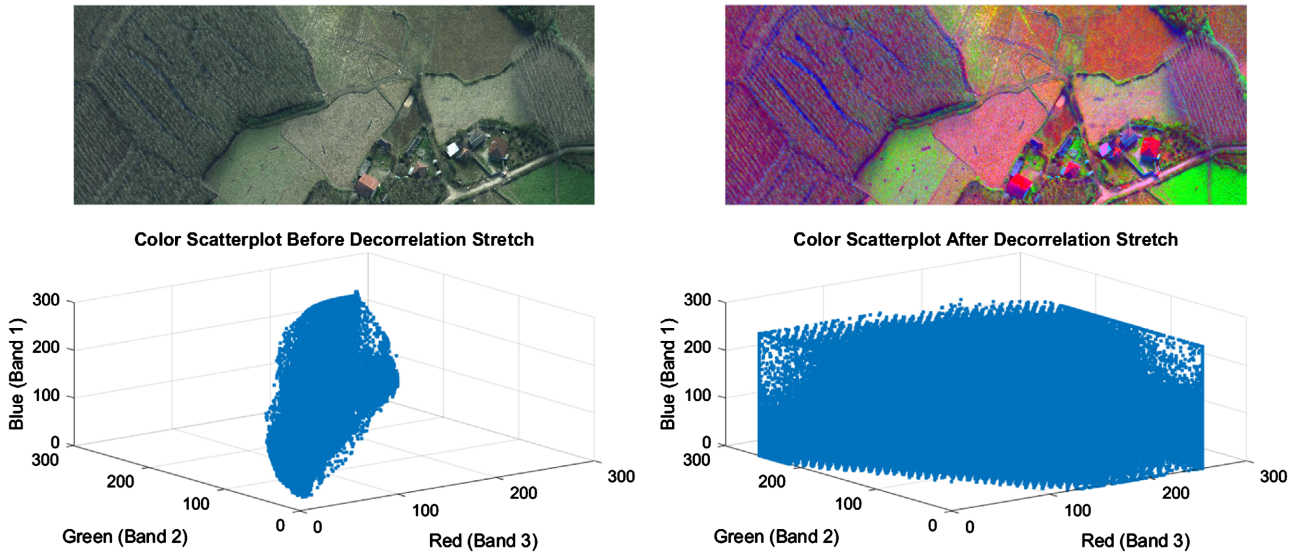

Figure 2. Image decorrelation stretching and enhancement of color separation including original image, decorrelation stretched image, color scatter plot before decorrelation stretch and color scatter plot after decorrelation strech

mean and variance in each band that is the same as the original RGB image (**Figure 2**).

2.3.1. Image Smoothing

A Gaussian filter was used to remove the noise in the RGB image. The one-dimensional Gaussian function is given by:

$$G(x,y)=\frac{1}{\sqrt{2\pi\sigma^2}}e^{\frac{-x^2}{2\sigma^2}} \tag{5}$$

where σ is the standard deviation, and x is the distance of the pixel from origin (**Figure 3(a)**). Following [17] the Gaussian filtering was done with filter size of 17 × 17 and 6 of 4 (**Figure 3(b)**).

2.3.2. Image Segmentation

After the decorrelation stretch and image smoothing, a high spatial resolution remote sensing image (Ultracam image) was converted into the Lab color space having three components including L, a, and b. The component of L represents gray-scale color space while the components of a and b represent color features. Segmentation was done using a SLIC algorithm that adapted a k-means clustering approach to efficiently generate superpixels. The number of superpixels for the image window of size 1000 × 600 pixels was selected 500 and a compactness of 10 such that SLIC adheres to boundaries well. The SLIC algorithm groups pixels into regions with similar values, reduces noise by increasing color differences, and improves the performance of the algorithm. This creates N cells to help delineate leafless poplar plantations from other features.

Stage 1: Non-poplar separation

Detection and identification functions and index algorithms were performed on the fall imagery in two main stages. Non-poplar LCs are included built up

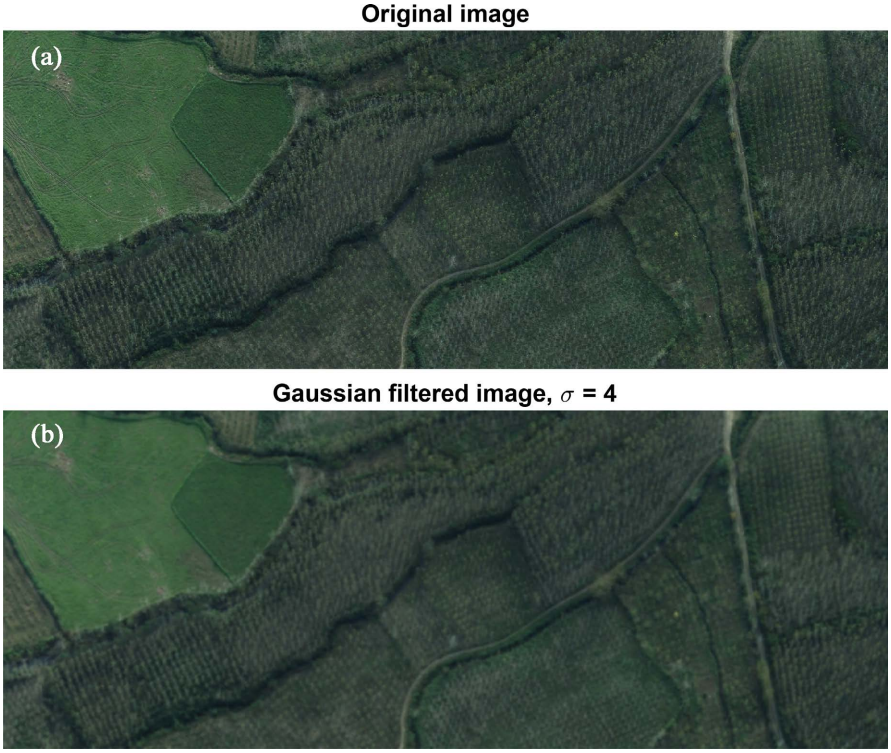

Figure 3. (a) Original image; (b) Gaussian filtered image obtained with filter size of 17 × 17 and 6 of 4

(e.g., road, roof, and boundaries), vegetation (e.g., agriculture and grass), and bare soil. There were spectral similarities between buildings, roof types, and leafless poplar trees as well as other urban targets such as roads and bare soil. Furthermore, areas with abandoned farms or young poplar plantation with weed coverage were difficult to differentiate from dense shrubbery land.

Given these challenges, seven different functions, indices, and statistical parameters were used to differentiate and exclude non-poplar cells in the fall imagery, which are described below.

Coefficient of Variation (CV)

Although CV (Equation (6)) has been used in various disciplines, it has not been applied to segregate some land cover types from poplar plantations. We employed the CV of red color to separate bare soil and several roof tops from leafless poplar plantations in the fall imagery. A threshold (T) was determined in the RGB processed image to segregate the similar red values. Setting a threshold creates binary images from grey level ones by turning all pixels of a cell that have a mean value below the threshold to zero. We determined different threshold values using the CV of each color.

$$\mathrm{CV_R} = \frac{\sigma_R}{m_R} \tag{6}$$

$$\sigma^2 = \sum_{i,j=0}^{N-1} p_{ij} \left(i - \mu\right)^2 \tag{7}$$

where $\mathrm{CV_R}$ is the coefficient of variation of red color, σ^2 is the variance of the in-

tensities of all reference pixels in the relationships that contributed to the GLCM.

Where σ_R is the standard deviation of values of red color intensity of pixels in a cell. m_R is the mean of red and so on for green and blue color.

$$m = \sum_{i,j=0}^{N-1} ip_{ij} \tag{8}$$

Here T of CV equals to 0.21 for red color. It is found that the red color acted as a classifier for the separation of bare soil and rooftops which are sufficiently uniform throughout the cell.

We set a suitable threshold of NGI (Equation (2)) that made it possible to distinguish green fields from grass in the poplar plantation (Table 1). Fall planting is common in our study area due to the climate and other characteristics. Because most of poplar trees lack leaves in the fall image, NGI appeared to successfully delineate green farms and gardens from leafless poplar plantations.

It is found that leafless poplar trees are star-shaped in the binary image. Hence an index that was defined with a histogram of white and black pixels was used.

$$F = \frac{N(1) - N(0)}{N(1) + N(0)} \tag{9}$$

where $N(1)$ and $N(0)$ are the number of white and black pixels respectively. To create this index, the RGB image was converted to gray scale, and then all pixels in the gray-scaled image with luminance larger than level 0.4 were replaced with the value of 1 (white) and all others set to 0 (black). By setting a threshold for the factor F (Equation (9)) (Table 1), we found that it was able to delineate some bare soil, roof, and road cells while the CV of red color could not.

It is found that the mean of NIR pixel values could delineate roads, green farms, and grasses. Spectral wavelengths corresponding to poplar trees have a peak in the NIR spectrum. We created a low and high limitation mean NIR range to capture different cover types.

NDVI (Equation (3)) can be used for detecting areas of forests, green farms, and grasses. However, there are grasses which appear within poplar plantations. We wanted to separate grass grown in poplar plantations from other green

Table 1. Threshold values of discriminators.

Discriminator	Threshold value
Mean homogeneity	$T > 0.7$
Grey level image to binary image	$T < 0.4$
CV_R	$T < 0.17$
NDVI	$0 < T < 0.3$
Histogram	$T < 0.7$
Mean blue	$15 < T < 150$
NRI	$T < 0.5$

vegetation such as forests and green farms, and set a threshold for mean NDVI values to identify highly vegetated land cover such as dense forest and uniformly green farms.

The study area contained a wide range of soil conditions. Consequently, several indices were required for soil detection. NRI (Equation (1)) was used for detecting soil and rooftop by setting its threshold to 0.5. Then, based on this threshold value, the cell was identified as poplar or non-poplar land cover.

The proposed approach was used an additional and efficient condition to detect non-poplar cells. The RGB image was converted to a different color space, HSV, which is defined with Hue, Saturation and Value channels. The value varies between 0 and 1 and shows the brightness. Our observation and examination showed that the histogram of value under a certain threshold, can separate bare soil and roofs from other land covers.

In the process of non-poplar separation, the number of cells which must be detected will decrease step by step. Since an LC and/or part of an LC was detected as non-poplar by a function or an index, that detected LC receives a zero code and will not be detected by other functions. Each function and index separated a portion of non-poplar into the non-poplar class.

Stage 2: Leafless poplar identification

After detecting and discarding non-poplar cells, an approach was developed for poplar identification in the remaining areas. We began by developing a procedure to detect leafless poplar plantations. As primary tools, texture and color features were chosen for poplar identification. When poplar trees are visually recognized in the fall imagery, it clearly appears as a periodic rough surface (a texture property) and gray-white color (a color property). Thus, we attempted to recognize both of these properties simultaneously in high spatial resolution imagery. Unlike the color, which is a single pixel-based property, texture properties are based on patterns in the area. For extraction of the color/texture features, RGB and HSV color spaces were employed. The most often used method to measure texture is GLCM. The GLCM is a two-dimensional histogram of gray levels for a pair of pixels which are separated by a fixed spatial relationship [18]. Since the poplar plantations have a wide range of age, the shapes of the crown and canopy of trees are very different. 15 different textures were identified within our study area and used a subset to identify leafless poplar plantations.

The grayscale image was converted to a binary form. As shown in **Figure 10**, leafless poplar trees in binary image (black and white pixels) are similar to a star shape. The function uses 1 pixel with 8 neighbor connectivity for two dimensional binary image to find connected white pixels. After finding the connected white pixels in the binary image and counting them in a cell, thresholding at some predetermined value is needed. Now, it can be obtained a poplar/non-poplar classification.

Gray Level Co-occurrence Matrix (GLCM) is a suitable algorithm to extract the texture features from the image of land-use regions with irregular shape [19].

In this paper, the potential of correlation and homogeneity functions (Equations (10) and (11)) were examined to identify leafless poplar plantations. Correlation function returns how a pixel is correlated to its neighbor over the GLCM cells. In other words, it can determine the linear dependency of gray levels on those of neighboring pixels.

Poplar trees are usually planted in an almost equal distance. To the best of our knowledge, the use of correlation analysis between adjacent pixels has not been used before to identify leafless poplar trees. The correlation between different neighboring pixels was investigated for poplar plantation and non-poplar land cover identification, given that some non-poplar cells were detected and excluded in previous processing stage. The correlation function is described below and was successful in identifying poplar plantations in a wide range of age classes due to the commonality of poplar features.

$$\text{Correlation} = \sum_{i,j=0}^{N-1} \frac{(I-\mu_i)(j-\mu_j)}{\sigma_i \sigma_j} p_{ij} \tag{10}$$

Homogeneity measures the closeness of the distribution of elements of the GLCM to the GLCM diagonal. A new use of homogeneity is proposed herein for identifying leafless poplar plantation in the fall image. Because the previous function may detect correlation in some plowed lands which confuses with poplar plantations, application of another property of texture (homogeneity) was useful for poplar identification.

$$\text{Homogeneity} = \sum_{i,j=0}^{N-1} \frac{p_{ij}}{1+|i-j|} \tag{11}$$

It is found that the blue image can be a discriminator of leafless poplar trees which have wide and intertwined crowns. Because leafless poplar trees (trunks and leafless crowns) have unique spectral characteristics in the blue spectrum of the RGB image. Simultaneous utilizing of thresholds of blue spectrum and NDVI had an effective role in identifying old poplar plantations in which the pattern of their regular cultivation was not clear in the aerial image. **Figure 4** illustrates the main stages of the method for separating non-poplar and identification of leafless poplar plantations.

2.4. Validation of New Method

After conducting all the above-mentioned steps, the final output image consists of two classes: poplar plantation and non-poplar. Each cell on the output image included visual information close to the visible image (RGB image). To assess the performance of the proposed methods and the classification accuracy, 145 cells were randomly selected within several windows of the input images. The type of LC of each cell in the output image was compared with the type of LC in the corresponding cell in the input image (RGB image) based on visual interpretation and field surveys. True and false classification was determined for each test cell in the selected windows of the output images. Classification accuracy of

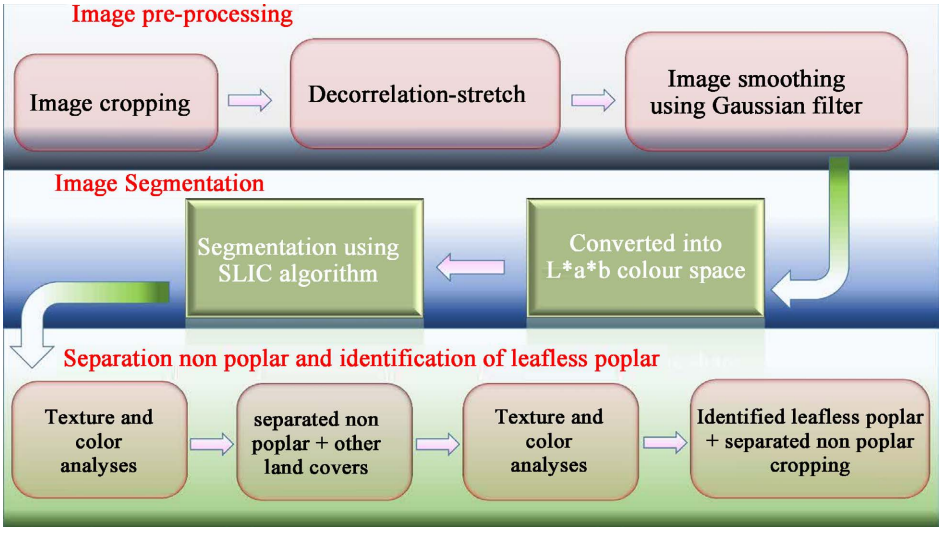

Figure 4. The main stages for separating of non-poplar and identifying leafless poplar plantation.

each class (poplar plantation and non-poplar) and the overall accuracy were computed.

3. Results and Discussion

Our primary objectives were to identify leafless poplar plantations as well as separating and excluding non-poplar areas. We used several different functions and discriminators to separate and remove everything that was non-poplar from the leafless poplar trees. In separating non-poplars, the intention was not to separate a specific land cover type from non-poplars at all. Conversely, our objective was developing the functions that could delineate several objects of non-poplar such as bare soil, rooftops, and roads simultaneously.

3.1. Non-Poplar Separation

We applied a set of discriminators including CV, NGI, *star-shaped feature*, NIR color, NDVI, NRI, and HSV to separate non-poplar from other land cover types in the fall imagery. Classified non-poplar is the combined result of applying all above mentioned statistical parameters, spectral and color indexes, and texture functions on the high spatial resolution imagery.

Segments relevant (**Figure 5(a)**) to a type of bear soil were filtered and separated by setting of an appropriate CV threshold of red color intensity (**Figure 5(b)**). The potential of CV (as a normalized measure of dispersion) for red color intensity in separation a type of bare soil from other land covers (e.g. leafless poplar trees) was clearly verified. Verification was accomplished by overlaying the differentiated bare soil on the RGB image (**Figure 5(a)** and **Figure 5(b)**). It was revealed that the red color acts as a classifier for the separation of a type of bear soil and several roofs which are sufficiently uniform throughout the cell. For example, the CV_R was 0.11 for a typical bare soil and 0.17 for a poplar plantation cell.

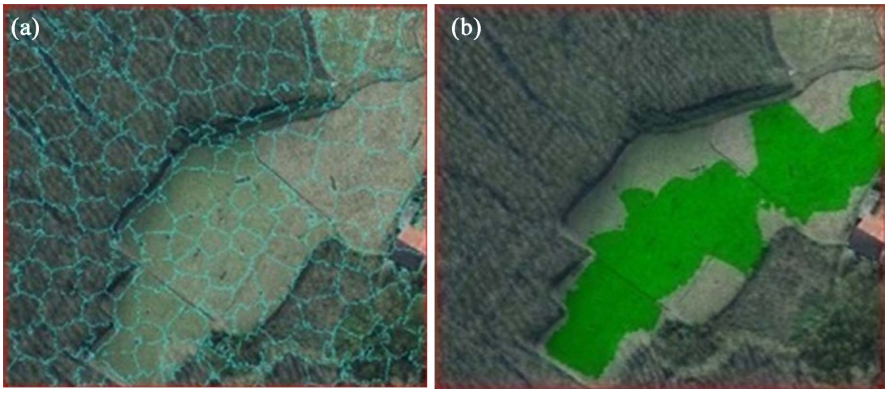

Figure 5. (b) Separated bare soil (colored part in the right side image) resulted from applying a CV threshold on the red color intensity that was overlaid on the RGB image. (a) is related to the corresponding segmented RGB image.

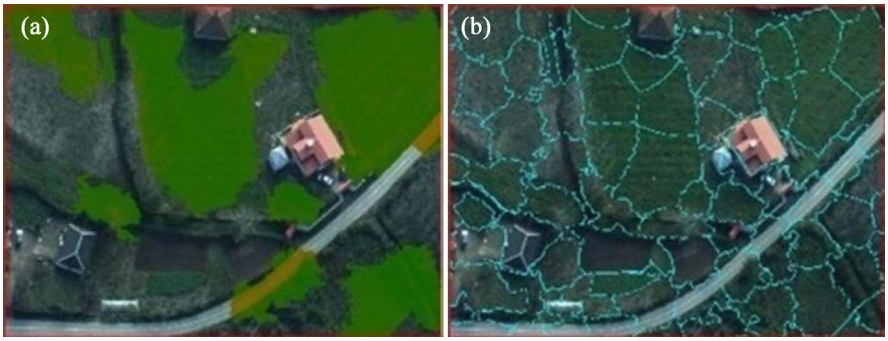

Figure 6. (a) Separated green farms and gardens (colored part in the right side image) resulted from applying NGI threshold that was overlaid on the RGB image. (b) is related to the corresponding segmented RGB image.

The results revealed the potential of an optimal threshold value on the cells of segmented NGI (**Figure 6(a)**) to exclude green farms and gardens from grasses that grow between poplar plantation lines (**Figure 6(b)**).

Star shaped feature has two functions. Here the luminance level in the gray-scaled image and the threshold for the factor F in function 9, as two components related to the star shaped feature, were impactful in successfully discriminating non-poplar land cover types such as bare soil, rooftops, and roads in the binary image (**Figure 7(a)** and **Figure 7(b)**).

The NDVI threshold value differentiated highly vegetated land such as dense forest and uniformly green farms from other LC (**Figure 8(a)** and **Figure 8(b)**).

The histogram of value, under a certain threshold, discriminated very effectively a considerable part of bare soil (**Figure 9(a)** and **Figure 9(b)**).

3.2. Identification of Leafless Poplar Plantation

After separating and excluding major non-poplar trees, leafless poplar identification was performed using a set of several functions, indexes, and color spectrums consisting of star shaped features, correlation, homogeneity functions, NDVI, and blue spectrum analyses. The combination of these processes and

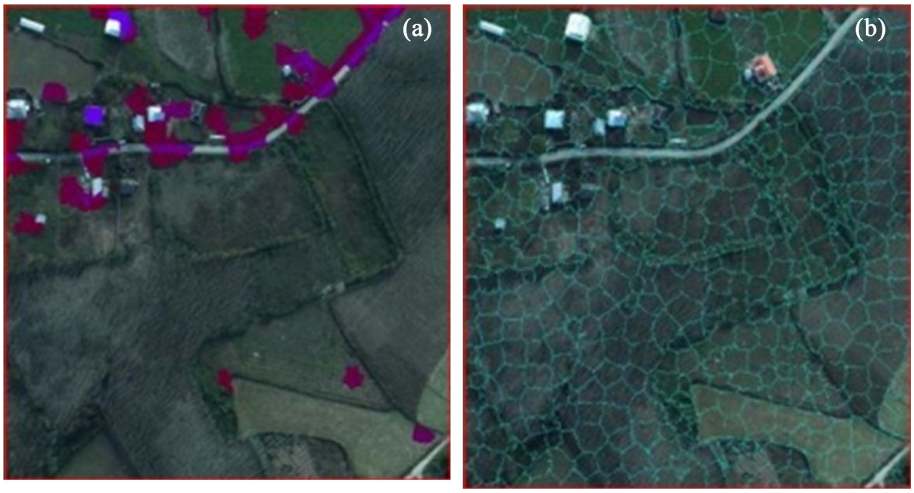

Figure 7. (a) Separated built-ups and bare soil (colored part in the right side image) resulted from applying function 9 threshold was overlaid on the RGB image. (b) is related to the corresponding segmented RGB image.

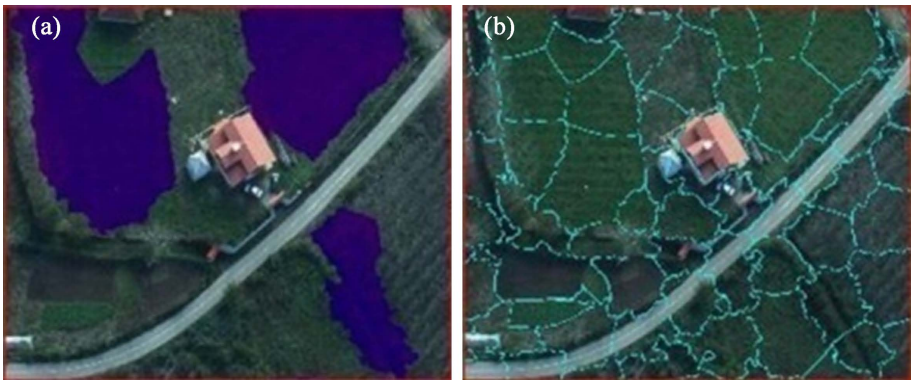

Figure 8. (a) Separated highly vegetated land cover (colored part in the right side image) resulted from applying an NDVI threshold that was overlaid on the RGB image. (b) is related to the corresponding segmented RGB image.

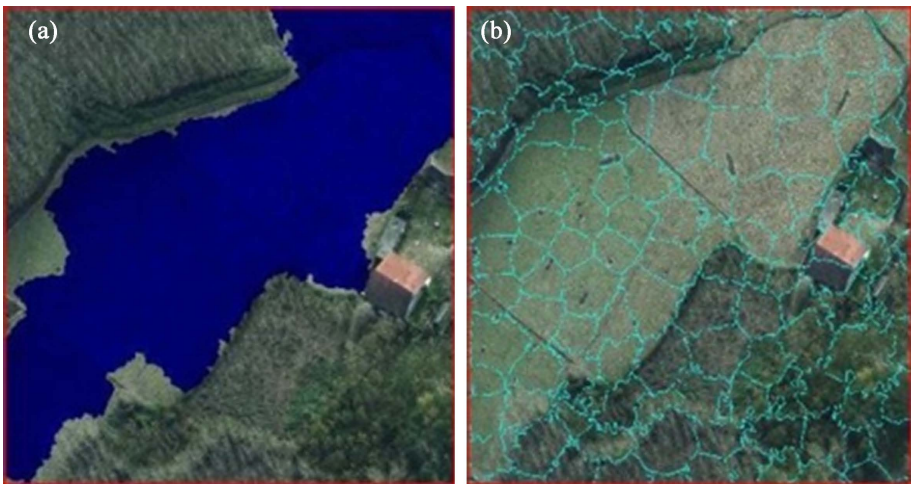

Figure 9. (a) Separated bare soil (colored part in the right side image) that resulted from applying a histogram of value that was overlaid on the RGB image. (b) is related to the corresponding segmented RGB image.

analyses created a classification of leafless poplar plantations and non-poplar land cover.

3.2.1. Star Shaped Feature

The star shape of leafless poplar trees in binary imagery (grayscale converted image) was a distinctive and powerful in identifying leafless poplar plantations (**Figure 10(a)** and **Figure 10(b)**). By using this characteristic, a significant part of the leafless poplar plantation was identified.

Identification of leafless trees and their differentiation from bare soil in fall imagery is a challenge in remote sensing. Distinguishing the star shaped feature of leafless trees in a binary image made it possible to identify leafless poplar plantations and to separate the bare soil, roof and road from other LCs (**Figure 11(a)** and **Figure 11(b)**).

3.2.2. Correlation Relationships

One of the helpful features we found was the correlation relationships between adjacent pixels in remote sensing imagery with high spatial resolution to identify leafless poplar plantations. This function revealed the correlation between pixels that were separated at consistent distances (**Figure 12**). Correlation between

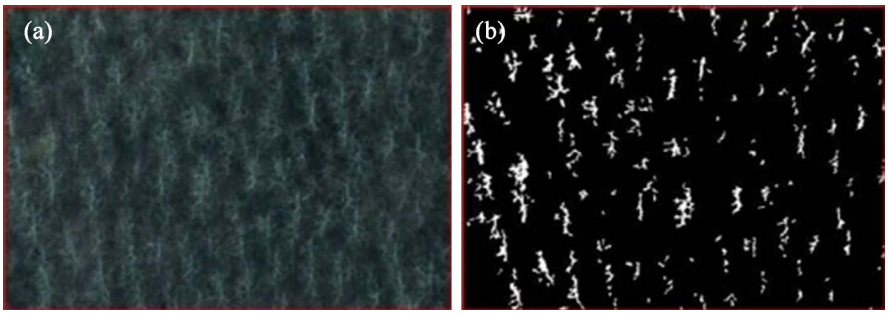

Figure 10. (a) and (b) which prepared from a region of the study area, are the windows of original and binary images respectively. (b) Star shape of the leafless poplar trees is completely clear in the binary image.

Figure 11. (a) Identified leafless poplar plantation (colored part in the right side image) resulted from applying star shaped feature was overlaid on the RGB image (b) is related to the corresponding segmented RGB image.

different neighboring pixels defined in the offset was dissimilar for leafless poplar plantation and non-poplar land covers. In a 1 to 40 pixels range, the correlation plot for poplar plantation had two maximum (15 and 35) and two minimum (10 and 25) offsets. This special periodic pattern was created by using the high spatial resolution imagery. Although this feature can appear in other land covers (e.g. plowed or planted land), the prominence (height of the peaks) and relative position of the peaks and the shape of the curve in correlation plot were remarkably distinctive for the leafless poplar plantation. Consequently, we found that the features extracted from correlation analysis of texture parameters can be used to distinguish leafless poplar plantations.

3.2.3. Homogeneity Function

The leafless poplar plantation areas had higher homogeneity when compared to plowed soil areas. This texture feature along with correlation analysis considerably increased our ability to separate leafless poplar plantation areas from plowed soil after determining a threshold on the homogeneity function and applying this threshold on the binary image (**Figure 13(a)** and **Figure 13(b)**).

3.2.4. Blue Spectrum

Leafless large poplar trees (trunks and leafless crowns) displayed special spectral characteristics in the blue spectrum in the fall imagery. This feature along with NDVI had observable importance in the separation of the poplar trees that had

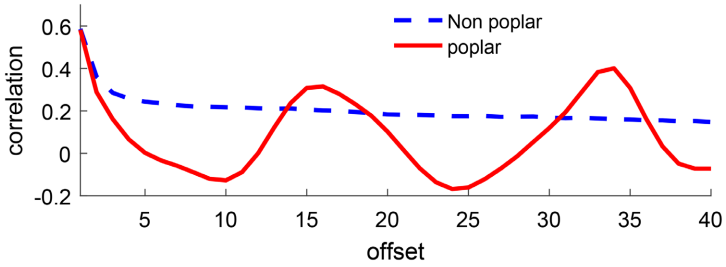

Figure 12. Correlation of an image includes poplar plantation and a bear soil vs offset.

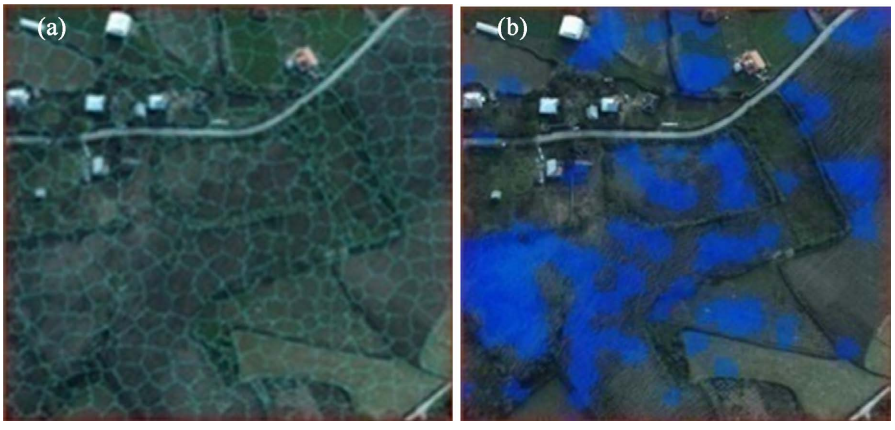

Figure 13. (a) Identified leafless poplar plantation (colored part in the right side image) that resulted from applying homogeneity function. (b) is related to the corresponding segmented RGB image.

intertwined crowns from other land covers (Figure 14(a) and Figure 14(b)).

Our overall classification accuracy result was 81.3% (Table 2). There is some classification accuracy concern between the non-poplar and the other land-cover classes with leafless poplar plantation. This problem was not completely resolved by using texture information and star shaped features. Star shaped features for leafless poplars along with other classifier algorithms employed in this study, successfully discriminated them from the other land cover types with an user accuracy of 84%. Our final classified product depicted leafless poplar plantations and non-poplar land covers. In viewing four regions within the study site (Figure 15), the texture-color classification appeared to separate leafless poplar plantations and non-poplar areas successfully.

Previous studies on leafless trees have tended to focus on segregating leafless trees and determining defoliation level of tree crowns. For instance, [1] classified full canopy and leafless trees in bottomland hardwoods using world view imagery. Reported user accuracy was around 82 %. Also, [2] obtained the overall classification accuracy of holm oak defoliation around 86% using a combination of multispectral WV-2 and ALS data with a Random Forest (RF) classifier. Similarly, [20] separated leafless trees from other objects without determination of the type of the tree. Our efforts to identify leafless poplar trees from surrounding land cover types resulted in a relatively high accuracy and provides a template for others to follow.

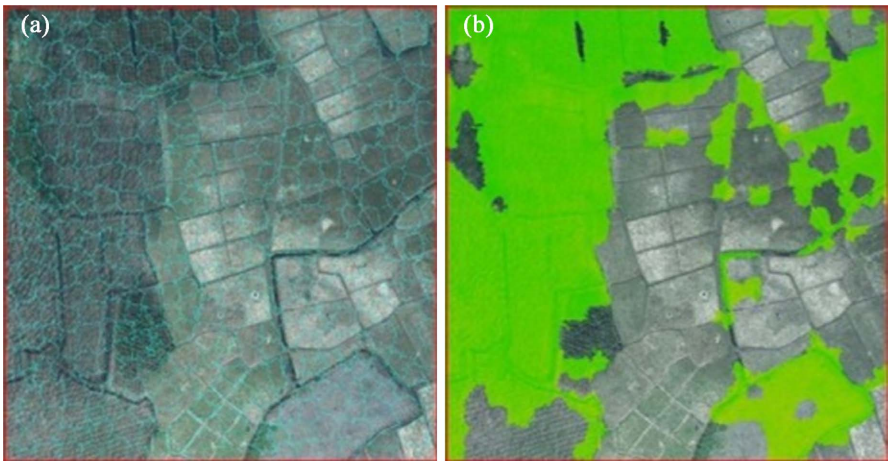

Figure 14. (a) Identified leafless poplar plantation (colored part in the right side image) resulting from applying blue color analysis. (b) is related to the corresponding segmented RGB image.

Table 2. Classification accuracy of leafless poplar plantation and non-poplar.

Class	Non-poplar	Leafless poplar	Unknown	Total	User Accuracy (%)	Overall Accuracy (%)
Non-poplar	76	5	14	95	80	81.3
Leafless poplar	3	42	5	50	84	

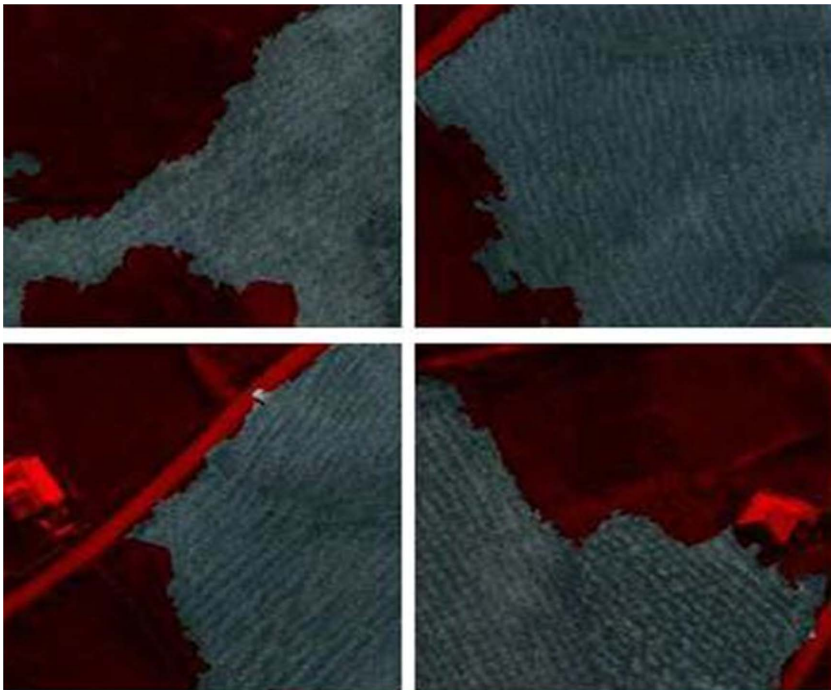

Figure 15. Final and enlarged classification result of the study area showing leafless poplar plantation (non-colored part) and non-poplar areas (colored part) respectively.

4. Conclusions

We successfully created a novel method to identify leafless poplar plantations based on their texture features and color properties. This method offers the possibility of identifying other leafless tree plantations with high resolution spatial imagery. We developed and assessed a set of functions, indices, and relevant optimal thresholds for differentiation of non-poplar land cover types and identifying leafless poplar plantations. Spectrally, differentiation of leafless trees from bare soil is challenging, and we employed star shaped features and the combination of functions such as homogeneity, correlation, and transfer and converter functions that enabled separation of these land cover types. The star shaped feature application in our analysis proved to be advantageous in our binary image analysis. This method provides a framework for identification of leafless poplar trees that may be beneficial for distinguishing other types of leafless trees.

Leafless poplar plantations which were located in a rural area, dominated most of the study area. Therefore, identification type of leafless trees in a forest area can be considered as complementary research.

Statements and Declarations

"The authors declare that no funds, grants, or other support were received during the preparation of this manuscript."

Data Availability

The datasets generated during and/or analysed during the current study are

available from the corresponding author on reasonable request.

Acknowledgments

We would like to thank Dr. Mohammadreaz Babaee, Dr. Masoud Tabari for their constructive comments and suggestions that greatly improve the manuscript. The present paper has been accomplished in due time owing to proper assistance of Mr. Masoud Nazifi.

Conflicts of Interest

The authors declare no conflicts of interest regarding the publication of this paper.

References

[1] Sapkota, B.B. and Liang, L. (2018) A Multistep Approach to Classify Full Canopy and Leafless Trees in Bottomland Hardwoods Using Very High-Resolution Imagery. *Journal of Sustainable Forestry*, **37**, 339-356. https://doi.org/10.1080/10549811.2017.1409637

[2] Navarro-Cerrillo, R.M., Varo-Martinez, M.A., Acosta, C., Rodriguez, G.P., Sanchez-Cuesta, R. and Gomez, F.J.R. (2019) Integration of WorldView-2 and AirborneLaser Scanning Data to Classify Defoliation Levels in *Quercus ilex* L. Dehesas Affected by Root Rot Mortality: Management Implications. *Forest Ecology and Management*, **451**, Article ID: 117564. https://doi.org/10.1016/j.foreco.2019.117564

[3] Gea-Izquierdo, G., Fernández-de-Uña, L. and Cañellas, I. (2013) Growth Projections Reveal Local Vulnerability of Mediterranean Oaks with Rising Temperatures. *Forest Ecology and Management*, **305**, 282-293. https://doi.org/10.1016/j.foreco.2013.05.058

[4] Singh, K.P. and Kushwaha, C.P. (2016) Deciduousness in Tropical Trees and Its Potential as Indicator of Climate Change: A Review. *Ecological Indicators*, **69**, 699-706. https://doi.org/10.1016/j.ecolind.2016.04.011

[5] Vaughn, N.R., Asner, G.P., Brodrick, P.G., Martin, R.E., Heckler, J.W., Knapp, D.E. and Hughes, R.F. (2018) An Approach for High-Resolution Mapping of Hawaiian Metrosideros Forest Mortality Using Laser-Guided Imaging Spectroscopy. *Remote Sensing*, **10**, Article 502. https://doi.org/10.3390/rs10040502

[6] Barrett, E.C. (2013) Introduction to Environmental Remote Sensing. 1st Edition, Routledge, London. https://doi.org/10.4324/9780203761038

[7] Khorrami, R., Naeimi, Z., Tabari, M. and Eslahchi, M.R. (2018) A New Method for Detecting Individual Trees in Aerial LiDAR Point Clouds Using Absolute Height Maxima. *Environmental Monitoring and Assessment*, **190**, Article No. 708. https://doi.org/10.1007/s10661-018-7082-8

[8] Kakooei, M. and Baleghi, Y. (2017) Fusion of Satellite, Aircraft, and UAV Data for Automatic Disaster Damage Assessment. *International Journal of Remote Sensing*, **38**, 2511-2534. https://doi.org/10.1080/01431161.2017.1294780

[9] Kakooei, M. and Baleghi, Y. (2020) VHR Semantic Labeling by Random Forest Classification and Fusion of Spectral and Spatial Features on Google Earth Engine. *Journal of AI and Data Mining*, **8**, 357-370.

[10] Li, Z.Q., Xu, D. and Guo, X.L. (2014) Remote Sensing of Ecosystem Health: Opportunities, Challenges, and Future Perspectives. *Sensors*, **14**, 21117-21139. https://doi.org/10.3390/s141121117

[11] Taufik, A., Syed Ahmad, S.S. and Ahmad, A. (2016) Classification of Landsat 8 Satellite Data Using NDVI Thresholds. *Journal of Telecommunication*, *Electronic and Computer Engineering*, **8**, 37-40.

[12] Giannini, M.B., Merola, P. and Allegrini, A. (2012) Texture Analysis for Urban Areas Classification in High Resolution Satellite Imagery. *Applied Remote Sensing Journal*, **2**, 65-71.

[13] Zhang, J. and Tan, T. (2002) Brief Review of Invariant Texture Analysis Methods. *Pattern Recognition*, **35**, 735-747. https://doi.org/10.1016/S0031-3203(01)00074-7

[14] Khokher, A. and Talwar, R. (2012) Content-Based Image Retrieval: Feature Extraction Techniques and Applications. *International Conference on Recent Advances and Future Trends in Information Technology* (*iRAFIT2012*), April 2012, 9-14.

[15] Tarika, B., Kaur, M. and Singh, I. (2014) Review of Histogram Equalization Techniques. *International Journal of Engineering and Computer Science*, **3**, 9205-9210.

[16] Liu. X. and Charrier, C. (2019) Can Image Quality Enhancement Methods Improve the Performance of Biometric Systems for Degraded Visible Wavelength Iris Images. 2019 3*rd Proceedings*, *International Conference on Bio-Engineering for Smart Technologies*, Paris, 24-26 April 2019, 119-122. https://doi.org/10.1109/BIOSMART.2019.8734200

[17] George, T., Potty, S.P. and Jose, S. (2014) Smile Detection from Still Images Using KNN Aalgorithm. 2014 *International Conference on Control*, *Instrumentation*, *Communication and Computational Technologies* (*ICCICCT*), Kanyakumari, 10-11 July 2014, 461-465. https://doi.org/10.1109/ICCICCT.2014.6993006

[18] Haralick, R.M., Shanmugam, K. and Dinstein, I. (1973) Textural Features for Image Classification. *IEEE Transactions on Systems*, *Man*, *and Cybernetics*, November 1973, 610-621. https://doi.org/10.1109/TSMC.1973.4309314

[19] Jiang, X., Wang, X. and Chen, D. (2018) Research on Defect Detection of Castings Based on Deep Residual Network. 2018 11*th International Congress on Image and Signal Processing*, *BioMedical Engineering and Informatics* (*CISP-BMEI*), Beijing, 13-15 October 2018, 1-6. https://doi.org/10.1109/CISP-BMEI.2018.8633254

[20] Krauß, T. (2019) Deriving Leafless Trees and Urban Structures from the DLR 3K Airborne Camera System for the City of Braunschweig. *Seventh International Conference on Remote Sensing and Geoinformation of the Environment* (*RSCy2019*) Paphos, Cyprus, 27 June 2019, 1117416. https://doi.org/10.1117/12.2534440